Implementation of one-way laser ranging observations into LRO into orbit determination.

S. Bauer[1], D. Dirkx[2], H. Hussmann[1], J. Oberst[1,3], D. Mao[4], G.A. Neumann[5], E. Mazarico[5l6], M.H. Torrence[7], J.F. McGarry[5], D.E. Smith[6], M.T. Zuber[6]. [1]DLR Berlin Germany, sven.bauer@dlr.de, [2]TU Delft, Netherlands,[3]TU Berlin, Germany, [4]Sigma Space Corporation, Lanham, MD USA, [5]NASA Goddard Space Flight Center, Greenbelt, MD USA, [6]MIT, Cambridge, MA USA, [7]SGT Inc., Greenbelt, MD USA.

Abstract

International Laser Ranging Service Ground Stations perform one-way laser ranging to NASA's Lunar Reconnaissance Orbiter which has operated in a lunar orbit since June 2009. We carried out precision orbit determination for LRO with one-way laser ranging observations only. We estimated LRO's initial state and clock as well as the clocks of the participating ground stations within a timeframe of 5 days. We use the nominal LRO orbit derived from radio data for assessing the orbit quality by comparing the retrieved trajectory and clock parameters. When we estimated the LRO initial state, clock and the ground station clocks over the 5 days, we saw a mean difference of 46.50 m with respect to the nominal trajectory. When we estimated the LRO clock every day within these 5 days this difference became 40.36 m. Furthermore we defined 4 arcs each with a ≈ 2-day length within the 5-day timeframe. By observing the differences of the results up to ≈ 1 day-long arc overlaps, we can perform an additional assessment of the orbit quality. At these overlaps we observed mean deviations of 21.20 m and an overall mean difference of 16.65 m w.r.t. the nominal trajectory.

Introduction and motivation

The one-way Laser Ranging (LR) experiment provides high-accuracy range measurements over lunar distances between International Laser Ranging Service (ILRS) ground stations and the Lunar Orbiter Laser Altimeter (LOLA) instrument onboard NASA's Lunar Reconnaissance Orbiter (LRO). Unlike ranging experiments to reflectors or transponder systems, LR to LRO is a one-way measurement. A ground station fires a laser pulse to LRO at a certain time and the received pulse is time stamped by the satellite. An optical receiver is attached to LRO's High Gain Antenna (HGA), which is always pointed towards Earth, and incoming laser pulses are transmitted into the LOLA laser detector by a fiber optic cable. This permits ranging measurements to LRO simultaneously while LOLA is ranging to the lunar surface for its primary altimetric purpose [1]. Because the receiver is attached to the HGA no further Earth pointing is required and this enables easy operation on the spacecraft (SC) side. By calculating the light travel time between the ground station and the satellite, a range measurement with a precision of typically 15 cm is derived for this experiment [2]. Currently the Precision Orbit Determination (POD) for LRO is based on traditional radio tracking as well as altimetric crossover data. This nominal trajectory is provided in the form of the LRO Spacecraft and Planet Ephemeris Kernel (SPK) with an accuracy around ≈ 10 m in total spacecraft position [3]. Knowledge of the LRO orbit, and the quality of the lunar remote sensing data products, are expected to improve with successful incorporation of the LR data to the LRO nominal navigation data [1]. Since the required extension of the SC segment is making use of the existing LOLA instrument and only adds a receiver and a fiber optic cable, the approach seems to be quite promising for missions who are supposed to have a laser altimeter on board. Thereby LR provides a more energy efficient tracking due to the more focused beam in comparison to radio tracking and will provide high bandwidth communication in future. The potential of LR for this has been already demonstrated with a two-way laser communications link at 622 Mbps from ground stations to the Lunar Laser Communications Demonstration (LLCD) instrument onboard NASA's Lunar Atmosphere and Dust Environment Explorer (LADEE) SC, which was thereby in orbit around the moon [4].

Table 1: Station specific LR data features

Station ID	Station Name	Location	Nr of passes	Nr of shots	NPT RMS in cm	Pass length in minutes
7090	YARL	Dongara, Western Australia, Australia	7	407	3.67	37
7110	MONL	Mt. Laguna, CA, USA	6	206	4.10	29
7125	GO1L	Greenbelt, Maryland, USA	17	529	8.13	49
		Total nr of passes and mean values	30	381	5.30	38

Method

We used the one-way LR observations to LRO processed previously [5] within the OD software ILR/Tudat [6] that derives a trajectory by adjusting the parameters of interest via a least squares optimization. We used Normal Point (NPT) data covering 5 days (26th until 30th of June 2010 or day 571 until 575 since 1st of January 2009). Within that period 3 stations were ranging to LRO for which related statistics are listed in Table 1. Figure 1 shows the tracking data coverage by station and the setup of 3 cases we defined for doing a variation of the state and the clock estimation. Thereby the first two cases (per-day and per-full-period) address the difference of estimating the LRO clock over short and long periods. Therefore we estimated the LRO clock every day ("per-day" - clock arc length of 1 day) and over the entire period ("per-full-period" - clock arc length of 5 days). The LRO state and the ground station (GS) clocks were always estimated over the whole period (LRO state arc length and GS clock arc length of 5 days). The third case used a length of up to 2 days for the arcs (LRO state and clock arc length as well as GS clock arc length of 2 days). The arc length was chosen so that we retrieve overlaps of up to one day. These overlaps are used to evaluate the quality and continuity of the derived trajectory by analyzing at the differences at those overlaps. Within the OD process we model both the LRO and the GS clocks with a 2nd order polynomial. The estimation of a bias, drift and aging for all involved clocks helped to remove trends and systematics from the measurement root mean square (RMS). We used the gravity field GRGM900C [7] from the GRAIL mission [8], which provides a high quality lunar gravity field on both the near and far sides. In order to keep the computation time and the accuracy at a reasonable level while performing many runs, we used the gravity field up to degree and order 180 (spatial blocksize = 30 km which is 1 degree). In this preliminary analysis we used a simple "cannonball" for modeling of solar radiation pressure. In this estimation we applied an area of 10m^2 and a radiation pressure coefficient of 1.2.

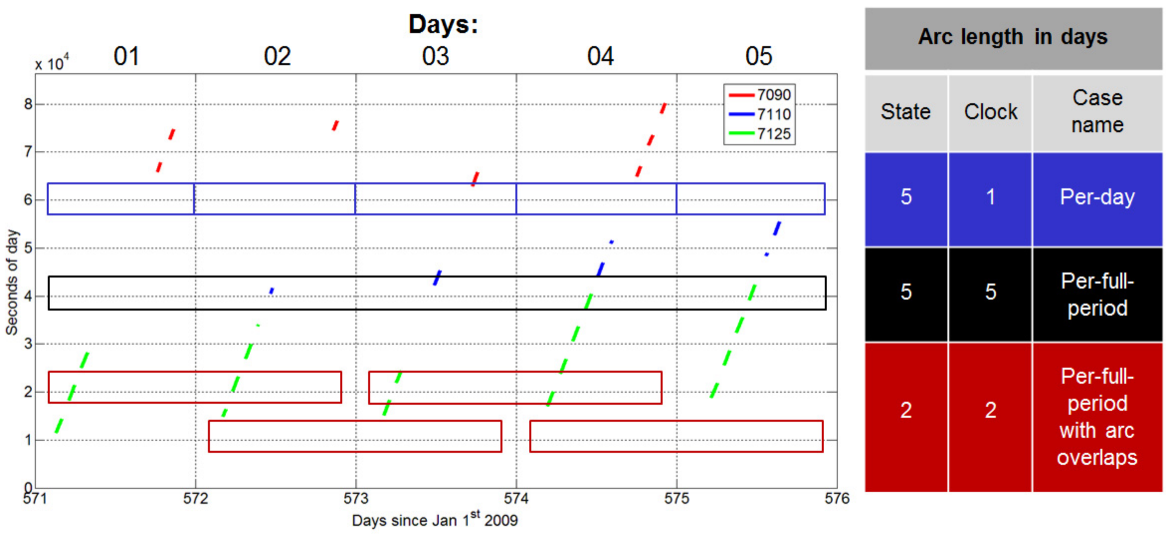

Figure 1: Distribution of LR data used in the analysis and setup of the defined cases

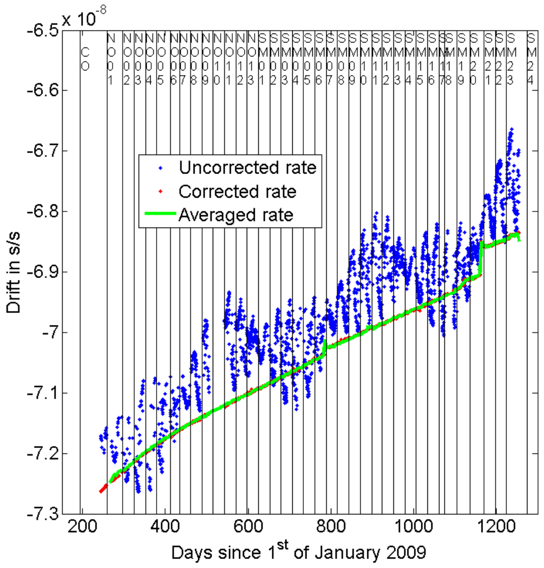

Figure 2: LRO clock rate w.r.t. TDB

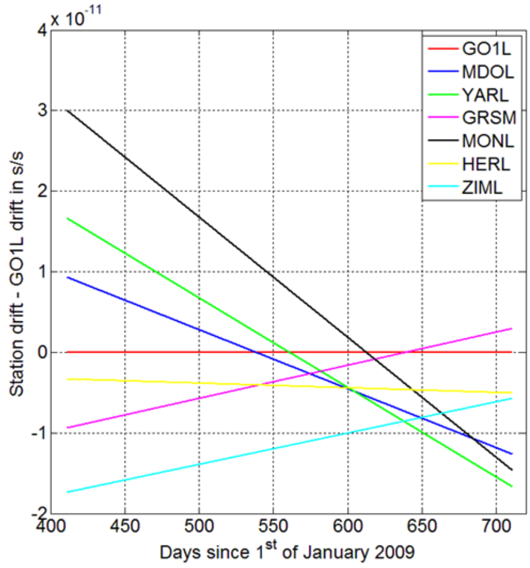

Figure 3: GS clock rates w.r.t. GO1L [2]

Due to the one-way setup, the state of LRO and the timing parameters of all clocks (LRO and all GS) need to be estimated simultaneously. Because the timing parameters are highly correlated, it is difficult to separate the effects of the involved clocks without further information. We provided *a priori* initial and σ (standard deviation) values on the state and the clocks within the OD processing, in order to estimate parameters of the initial state (leading to the trajectory) and all clocks. The information on the LRO clock was derived from our SPK-based analysis of the LRO one-way LR data. By using the fire time of a station and a predicted receive time derived with the LRO nominal trajectory, we can reference an actual receive event at LRO to that and obtain the one-way measurement. If we analyze the deviations of the receiving events in Barycentric Dynamical Time (TDB) and LRO's Mission Elapsed Time (MET), we can estimate the behavior of the LRO clock. The LRO clock rate w.r.t. TDB throughout the mission time is shown in Figure 2, whereby the rate is estimated on a per LR pass basis. The blue rate represents the raw MET rate of the clock w.r.t. TDB, without corrections for relativistic effects. The variation of the clock rate due to those effects can be identified by the variations with periods of 1 year, 28 days and the orbital period of ≈ 120 minutes. The red rate, with an over 3 days averaged green rate on top, is corrected for relativistic effects and allows for a direct analysis of the clocks aging process. The initial value of the LRO clock drift was set to 7.111×10^{-8} s/s and for the aging it was set to 4×10^{-17} s/s^2 – derived from the long-term trend of the drift. By observing the variation of the LRO clock rate w.r.t. the average rate we derived *a priori* σ values. The LRO clock analysis was also used for the evaluation of the estimated parameters, as it will be shown in the results.

In order to provide information on the GS clocks to the estimation, we used the difference between the GS clock rates w.r.t. GO1L (compare Figure 3). Since those values are differences in rate relative to the GO1L station rate and no total values, no initial *a priori* values were provided in the estimation. By using the range of the differences in rate, *a priori* σ values were derived for the GS. Since we know the GS clocks much less than the LRO clock, their *a priori* σ constraints were set less tight than for the LRO clock.

Results: 5 days, per-day and per-full-period

The results on the trajectory and the estimated parameters for the per-day (LRO state and GS clock arc length of 5 days, LRO clock length of 1 day) and per-full-period (LRO state, clock and GS clock arc length of 5 days) case are given in Table 2.

Table 2: Results of the per-day and per-full-period case

			Per-day	Per-full-period
Difference to the nominal trajectory	Mean in m		40.36	46.50
Difference in between	Mean in m		6.47	
RMS w.r.t. trajectory	Mean in m		1.10	2.27
LRO clock	Offset in s		$+1.1222\pm1.9818x10^{-03}$	$+2.0678x10^{-04}$
	Drift in s/s		$-7.1100\pm0.0003x10^{-08}$	$-7.1110x10^{-08}$
	Aging in s/s^2		$-6.7141\pm6.3264x10^{-17}$	$-2.9337x10^{-15}$
GS clock	Offset in s for station	7110	$-7.7916x10^{-05}$	$+2.0507x10^{-04}$
		7125	$-7.7499x10^{-05}$	$+2.0528x10^{-04}$
		7090	$-7.3023x10^{-05}$	$+2.0365x10^{-04}$
	Drift in s/s for station	7110	$-4.1653x10^{-12}$	**$+3.4784x10^{-13}$**
		7125	$-7.3567x10^{-12}$	**$+8.4757x10^{-13}$**
		7090	$-4.4276x10^{-11}$	**$+1.1063x10^{-11}$**
	Aging in s/s^2 for station	7110	$-3.0599x10^{-17}$	$-2.9510x10^{-15}$
		7125	$-2.3761x10^{-17}$	$-2.9529x10^{-15}$
		7090	$+4.7019x10^{-17}$	$-2.9704x10^{-15}$

Since for the per-day case 5 parameters are estimated, the values in Table 2 represent an average of those values, listed with their standard deviation. To evaluate the quality of the orbits we calculated the difference of the derived trajectories w.r.t. the GRGM900c-based orbit[1]. The difference of the derived trajectory is 40.36 m for the per-day case and 46.50 m for the per-full-period case. Because the difference is only 6.47 m when changing the clock arc length from 1 to 5 days, we assume that the errors from the dynamical models are more dominant over those from the clock model.

Figure 4 and Figure 5 show the RMS of the measurements of the three stations w.r.t. the derived trajectory for the per-day and the per-full-period case, respectively. As listed in Table 2 the mean value over the 5 days is 1.10 m for the per-day and 2.27 m for the per-full-period case. Since the measurement RMS only provides information about the orbit precision, it cannot be used to evaluate its accuracy. Hence the official LRO ephemeris, also a POD product on LRO, provides a more reliable and independent basis for evaluating the orbit quality. The per-day RMS is smaller and the residuals show smaller systematics and trends over the timeframe, since the LRO clock is estimated every day and therefore can absorb dynamical and clock errors (compare Figure 4 and Figure 5). Even though the per-day RMS values are larger, one might prefer longer clock arcs, depending on the type of parameters of interest one estimates. If the LRO clock is estimated too often, the strength of the parameters of interest might be reduced, resulting in a less correct solution [9].

Figure 6 shows the estimated LRO clock drift parameters w.r.t. the results from the SPK-based analysis. As visible both for the per-day and the per-full-period case, the estimated clock values agree with the values from the SPK-based analysis. While the per-day values show a scatter of $\approx 6.0x10^{-12}$ s/s w.r.t. a linear fit, the values from the SPK-based analysis have a variation of $\approx 7.6x10^{-12}$ s/s w.r.t. a linear fit.

[1] We used the orbit LRO_NO_12_20131125_GRGM900C_L600 from [10] for the comparison.

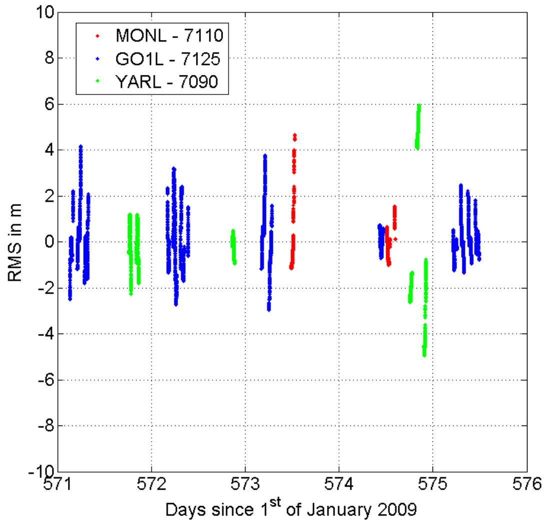

Figure 4: Measurement RMS w.r.t. the trajectory for the per-day case

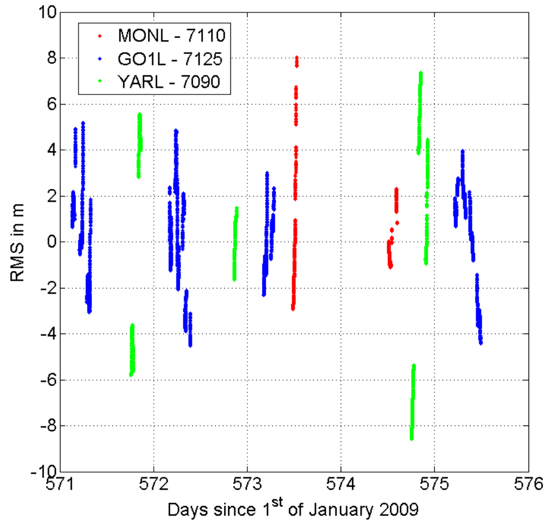

Figure 5: Measurement RMS w.r.t. the trajectory for the per-full-period case

By applying *a priori* information for the LRO and the GS clock, we were able to separate the correlated influences of the clocks and make sure to retrieve reasonable timing parameters. By setting the *a priori* σ values tighter for the LRO than for the GS clock, we make sure to only constrain well-known parts properly and not to bias our estimation.

While the estimated LRO clock drift rate agrees rather well with the values from the SPK-based analysis, the aging values differ significantly from the long-term value from the SPK-based analysis of 4×10^{-17} s/s^2. The short timeframe of 5 days, the correlated influences of the GS clocks and the dynamical errors are assumed to be the reason for that. That is indicated by the larger systematics and the larger difference w.r.t. the nominal LRO trajectory of the per-full-period case (see Figure 4, difference of 40.36 m on average) compared to the per-day case (see Figure 5, difference of 46.50 m on average). Evaluating the results of the GS clocks (also see Table 2) is more difficult, since we had no total values available from our work or in the literature for comparison. Therefore we estimated the difference of the estimated GS clock drifts of the stations YARL and MONL w.r.t. GO1L (see Table 3) in order to do a comparison to the values shown in Figure 3. The values used for calculating the difference in rate between the stations w.r.t. GO1L for the per-full-period case in Table 3 are thereby highlighted with red in Table 2. Both GS clock drifts w.r.t. GO1L differ from the results in shown Figure 3 by a factor of ≈ 10. This is caused by the different length of the GS clock analysis - while we estimated the GS clocks over 5 days, the results in Figure 3 averaged the GS clocks over the year 2010. Furthermore our estimated GS clock values do not necessarily represent the true clock behavior since they might have absorbed errors and correlated influences due to the usage of one-way LR observations only.

Table 3: Difference of the station drifts w.r.t. GO1L for the per-full-period case

Difference in drift for station combination	05 days OD	Results
7125/GO1L – 7110/MONL	5×10^{-13} s/s	6×10^{-12} s/s
7125/GO1L – 7090/YARL	1×10^{-11} s/s	1×10^{-12} s/s

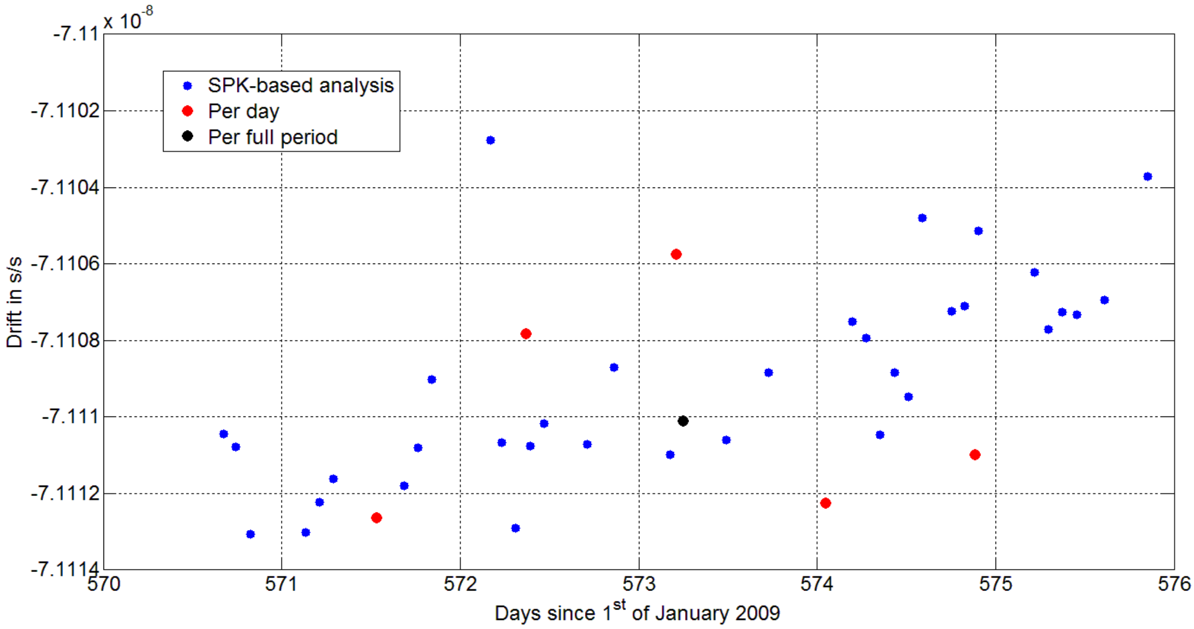

Figure 6: Estimated LRO clock rate for the two cases w.r.t. the results from the SPK-based analysis

Results: 2 days per-full-period with arc overlaps

For further investigation of the orbit quality and continuity we set up 4 arcs with a 2-day length each over the 5 days, such that there are overlaps of up to 1 day. By observing at the differences at the arc overlaps the consistency of the orbit itself can be checked. Previous work on polar lunar orbits ([11], [12] and [13]) found that a good compromise between sensitivity to gravity and contained compounded modeling errors was to conduct POD over 2.5-day arcs. We chose a length of 2 days in order to reasonably split the observation data within the 5 days. Table 4 lists the setup of the arcs, the difference of their trajectories w.r.t. the nominal trajectory, as well as the resulting overlaps and their difference. Figure 7 shows these differences and Figure 6 the estimated LRO clock drift w.r.t. the rates from the SPK-based analysis. During such a 2-days arc the LRO state and clock as well as GS clock were estimated once. While the measurement RMS values vary between 0.85 m to 1.27 m, the differences of the arc overlaps range from 17.78 to 25.68 m.

Table 4: Results for the 2-day cases with arc overlaps

<table>
<tr><th></th><th>Unit</th><th colspan="2">01 - 02</th><th colspan="2">02 - 03</th><th colspan="2">03 - 04</th><th colspan="2">04 - 05</th></tr>
<tr><td>Difference to the nominal trajectory</td><td>m</td><td colspan="2">10.96</td><td colspan="2">17.72</td><td colspan="2">28.93</td><td colspan="2">8.64</td></tr>
<tr><td>RMS w.r.t. trajectory</td><td>m</td><td colspan="2">1.27</td><td colspan="2">0.44</td><td colspan="2">1.52</td><td colspan="2">0.85</td></tr>
<tr><td>Overlap at day</td><td>day</td><td></td><td colspan="2">02</td><td colspan="2">03</td><td colspan="2">04</td><td></td></tr>
<tr><td>Arc overlap difference</td><td>m</td><td></td><td colspan="2">25.68</td><td colspan="2">20.13</td><td colspan="2">17.78</td><td></td></tr>
</table>

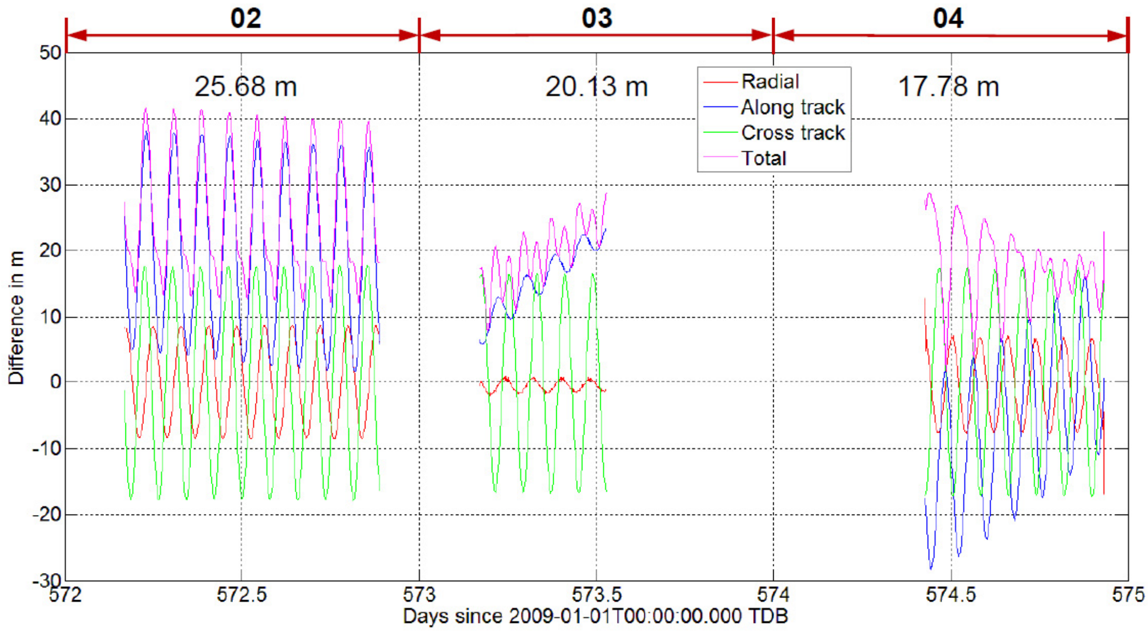

Figure 7: Differences at the arc overlaps

This result agrees with the differences to the nominal trajectory, which range from 8.64 to 28.93 m. This combined with the lack of jumps in the overlaps, shown in Figure 7, are collectively interpreted as an indicator of good orbit quality. The largest deviations are thereby on the along-track component, which is typically observed within the OD process.

Additionally, we compared the estimated LRO clock rates with the rates of the SPK-based analysis as shown in Figure 6. The values are in good agreement, while the estimated rates have smaller scatter (≈ 2.0×10^{-12} s/s) than the rates from the SPK-based analysis (≈ 7.6×10^{-12} s/s) w.r.t. a linear fit.

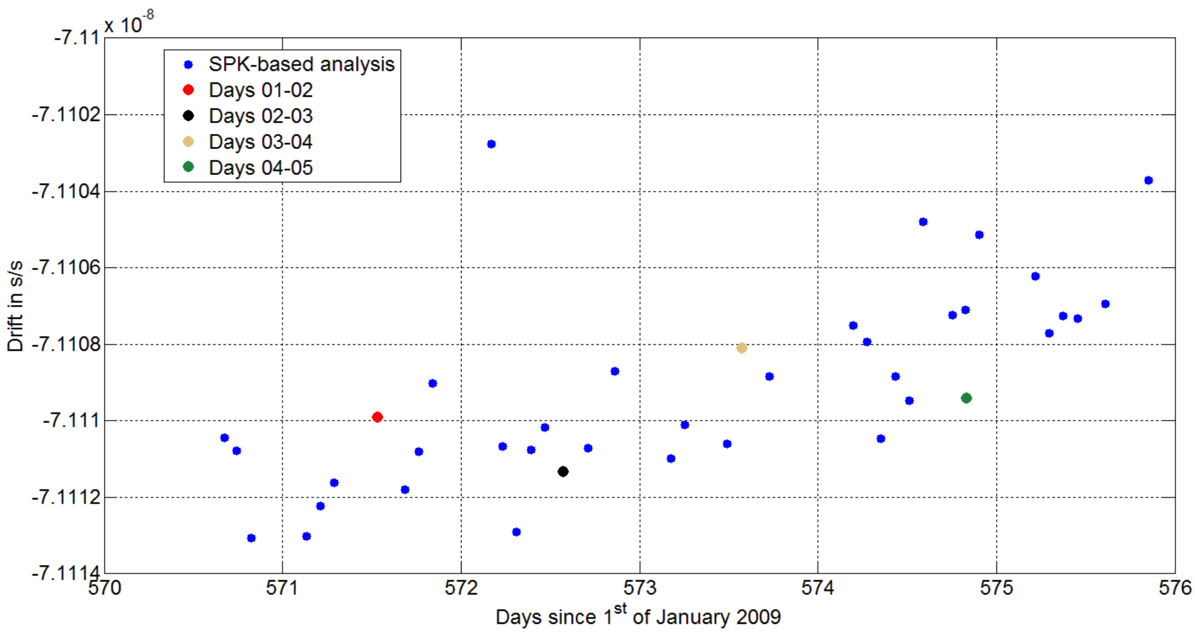

Figure 8: Estimated LRO clock rate for the 2-day case w.r.t. the results from the SPK-based analysis

Discussion and Summary

We carried out an OD for LRO while using only one-way LR data throughout the timeframe from the 26th until 30th of June 2010. We used the SPK-based analysis and literature in order to develop and provided *a priori* information and the assessment of the estimated parameters and trajectories. The *a priori* information enabled the separation of LRO and GS clock to some extent and thus the estimation of both reasonable timing parameters and trajectories. We defined various cases to check on the performance of our estimation, whereby we changed the LRO state and clock as well as the GS clock arc length. We compare the derived trajectory w.r.t. the nominal trajectory for getting a reliable evaluation of the orbit quality, since that is an OD from different data sets (radio and crossover) and thus the best independent result available. When we estimated the LRO state and the GS clock over 5 days, while estimating the LRO clock every day, we observed a mean difference to the nominal trajectory of 40.36 m. When estimating the LRO state, the clock as well as the GS clock over 5 days we observed a mean difference of 46.50 m w.r.t. the nominal trajectory. We further defined arcs with a 2-day length of the LRO state and clock as well as GS clock arcs, such that we retrieve overlapping trajectories. The average difference to the nominal trajectory is 16.65 m over the 5 days from the 4 arcs and their mean difference at the overlaps is 21.20 m. For this preliminary OD analysis, carried out with one-way LR data only, the observed deviations agree at the order of magnitude with the reported accuracy of the nominal trajectory of ≈ 10 m while the timing parameters look reasonable within the comparisons.

Future work

Since we observed variations of the trajectories w.r.t. the nominal trajectory and at the overlaps, with their largest component in the along-track direction, we intend to incorporate the estimation of empirical acceleration as a next step. Further, in order to account for the changing influence of solar radiation pressure due to changing geometry, we intend to estimate the solar radiation pressure coefficient. By further exploiting the SPK-based LRO clock analysis we intend to optimize the estimation of the timing parameters. Finally we wish to analyze data beyond a timeframe of only 5 days within the OD for LRO.

Acknowledgements

This work has been supported by the DFG (German Science Foundation). S. Bauer and D. Dirkx were also supported by the ESPaCE project, EC FP7 Grant Agreement 263466.

References:

[1] Zuber, M.T., et al.: The Lunar Reconnaissance Orbiter Laser Ranging Investigation, Space Sci Rev, 150, 63 – 80, 2010.

[2] Mao, D., et al.: Laser Ranging Experiment on Lunar Reconnaissance Orbiter: Timing Determination and Orbit Constraints, http://cddis.gsfc.nasa.gov, 17th International Workshop on Laser Ranging, 16-20 May 2011, Bad Kötzting, Germany 2011.

[3] Mazarico, E.,et al.: Improved Orbit Determination Of Lunar Orbiters with Lunar Gravity Fields Obtained, 23rd AIAA Space Flight Mechanics Meeting, 13-274, 10-14 February 2013, Kauai, HI, 2013.

[4] NASA, release 13-309, 22 October 2013: http://www.nasa.gov/press/2013/october/nasa-laser-communication-system-sets-record-with-data-transmissions-to-and-from, February 2014

[5] Bauer, S., et al.: Reduction and analysis of one-way laser ranging data from ILRS ground stations to LRO, http://www.congrexprojects.com/2013-events/13a06, 6th ESA International Workshop on Tracking, Telemetry and Command Systems for Space Applications (TTC), 2841662, 10-13 September, Darmstadt, Germany 2013.

[6] TU Delft: http://tudat.tudelft.nl, September 2014.

[7] Lemoine,F.G., et al.: GRGM900C: A degree 900 lunar gravity model from GRAIL primary and extended mission data, Geophys. Res. Lett., 41, 3382–3389, 2014.

[8] Zuber, M.T., et al: Gravity Recovery and Interior Laboratory (GRAIL): Mapping the lunar interior from crust to core, Space Sci. Rev., 178, doi: 10.1007/s11214-012-9952-7, 2013.

[9] Dirkx, D., et al.: Simulated Comparative Analysis of One- and Two-Way Planetary Laser Ranging Systems, http://ilrs.gsfc.nasa.gov, 19th International Workshop on Laser Ranging, 3101, 27-31 October 2014, Annapolis, MD, USA, 2014.

[10] LRO Radio Science PDS archive, http://pds-geosciences.wustl.edu/lro/lro-l-rss-1-tracking-v1/lrors_0001/data/spk, release #7 from 2014-12-15, February 2015

[11] Mazarico, E., et al.: Orbit determination of the Lunar Reconnaissance Orbiter, J. Geod., 86, 193-207, 2012.

[12] Mazarico, E., et al.: GLGM-3: A degree-150 lunar gravity model from the historical tracking data of NASA Moon orbiters, J. Geophys. Res., 115, doi:10.1029/2009JE003472, 2010.

[13] Konopliv, et al.: Recent Gravity Models as a Result of the Lunar Prospector Mission, Icarus, 150, 1-18, 2001.